A NEW EXACT ANALYSIS FOR ANISOTROPIC CONDUCTIVE HEAT TRANSFER IN TRUNCATED COMPOSITE SPHERICAL SHELLS

M. Norouzi*

Faculty of Mechanical Engineering
Shahrood University of Technology
Shahrood, Iran

H. Rahmani

Faculty of Mechanical Engineering
Amirkabir University of Technology
Tehran, Iran

A. K. Birjandi

Faculty of Mechanical Engineering
Shahrood University of Technology
Shahrood, Iran

ABSTRACT

In the present paper, a general analytical solution is proposed for anisotropic heat conduction through truncated composite spherical shells. The solution is so important in designing the spherical vessels which are usually used to store the CNG, LNG, LPG and other petroleum condensates. Herein, it is supposed that the fiber angle of composite laminate is in range of zero to 90 degrees. Heat convection with ambient flow, an external heat radiation, and a possible internal heat generation are modeled within the heat transfer equation. The exact solution is derived using the complex finite Fourier transform method. The particular solution of transferred equation is found based on the Green's function and Sturm-Liouville theories. Finally, an inverse integral transformation is applied to form the final analytical solution in physical space. Defining four materials differing in the value of conductivity coefficient in fiber direction, the effects of used composite material and fiber angle on temperature distribution of the spherical shell are investigated in detail.

Keywords: Analytical solution, Anisotropic heat conduction, Truncated composite spherical shell, Composite spherical vessel.

1. INTRODUCTION

The history of composite materials dates back to ancient times for construction applications but today they have remarkably attracted researchers to study their major features allowing them to be used in many industrial applications. Numerous features of composite materials such as high ratios of strength and stiffness to density, high corrosion resistance, and plasticity, make them reliable materials in various applications. Piping, pressure vessels, fluid reservoirs, aerospace elements, naval structures, beams, combustion chambers and chemical industry utilities are among the many applications of composite materials in today's industry. In contrast to mechanical properties of composite materials, their heat transfer behavior has been less studied [1-7]. Study on the heat transfer phenomena in composite materials provides valuable knowledge in many other applications such as analyzing fiber placement in the production process [8-10], preventing thermal fracture [11-13] and controlling the directional heat transfer in laminates.

Numerical approaches beside analytical methods are frequently used in the solution of heat conduction in a composite medium, however, because of the anisotropy exists in the physics of the problem, provision of numerical solutions seems more straightforward. Besides, novel developments in computational sciences make the numerical methods effective tools in thermal modeling [14-16]. However,

* Corresponding author (mnorouzi@shahroodut.ac.ir)

DOI : 10.1017/jmech.2018.54
Copyright © 2019 The Society of Theoretical and Applied Mechanics
https://doi.org/10.1017/jmech.2018.54 Published online by Cambridge University Press

analytical solutions provide direct insight into physical processes and highlight how thermal behavior can be governed by the parameters of the system which are essential for design and optimization phases [17].

There are several analytical solutions for unsteady heat conduction in 2-D composite materials [18-21]. The response of a 2-D multi-layer composite slab, to a sudden temperature change, has been analyzed by Salt [22, 23]. His analytical investigation was carried out in two- and three-layer composite slabs. Miller and Weaver [24] predicted the temperature distribution of composite material through a multi-layered system subjected to complex boundary condition. The system is exposed to convective and radiative boundary conditions. They used the separation of variables method and verified their solution with numerical results under the same boundary condition. A new simple refined computational model was presented by Blanc and Touratier [25] for heat conduction in multilayered composite laminates based on an equivalent single layer approach which allows to satisfy both continuity condition for temperature and the heat flux at the interfaces. According to this study, the effect of their approach on two and three dimensional heat conduction problems in comparison with exact calculation is investigated.

An analytical solution is developed by Ma *et al*. [26, 27] to determine the heat conduction in an anisotropic single layer [26] and multi-layered [27] media. They transformed an anisotropic to an isotropic problem by linear coordinate transformation. Norouzi *et al*. [28] presented an exact analytical solution for anisotropic heat conduction in composite cylindrical shell. The separation of variables method is used to solve the heat conduction equation and the unknown coefficients are determined by an efficient Fourier series-based technique. A Fourier transformation has been developed for steady and unsteady analytical solution by Kayhani *et al*. [29-31] and Amiri Delouei *et al*. [32] for axisymmetric heat conduction in cylindrical multi-layer composite laminates. The Meromorphic function method was employed to find the transient temperature distribution in laminate. There are also some studies investigated the conductive heat transfer in cylinders that made from a functional graded material and composite laminate [33, 34].

Among few studies that considered heat conduction of spherical multi-layered materials, Singh *et al.* [35] developed an analytical two-dimensional solution by using separation of variables method. Jain *et al.* [36] is also proposed an analytical unsteady solution for heat conduction in r–θ spherical coordinates for any combination of inhomogeneous boundary conditions at the inner and outer radial boundaries of the concentric layers. It must be noted that this solution is valid only for multi-layer spheres and cannot apply for multi-layer reinforced composites spheres. Kayhani *et al.* [37] studied the asymmetric steady-state heat conduction in cylindrical composite laminates. They used separation of variables method to solve the partial differential equation. The solution obtained is only valid for long pipes and vessels.

An exact analytical solution for unsteady heat conduction in cylindrical composite laminate was proposed by Norouzi *et al.* [38]. The Laplace transformation is used to derive anisotropic conductive heat transfer equations in the frequency domain, to which they applied the separation of variables method. Norouzi *et al.* [39] is also presented an exact analytical solution for steady-state conductive heat transfer in multilayer spherical fiber reinforced composite laminates. They used separation of variables method in order to investigate the heat conduction when general boundary conditions were applied inside and outside the laminate and the recursive Thomas algorithm is used to solve the final set of equations related to the coefficient of Fourier-Legendre series of temperature distribution.

Solution of heat conduction problem in composite conical shells is proposed by Norouzi and Rahmani [40, 41] for steady-state and transient cases. The steady-state solution used both canonical mapping and separation of variables methods to present the temperature distribution of composite conical shell. However, in transient case, the integral transform method is used and then the separation of variables method applied to solve the transferred equation.

In the present study, a general analytical solution is proposed for anisotropic heat conduction through truncated composite spherical shells for the first time. The fiber angle might have variety of values ranging from zero to 90 degrees. Heat convection with ambient flow, an external heat radiation, and a possible internal heat generation are modeled within the heat transfer equation. Defining four materials differing in the value of conductivity coefficient in fiber direction, the effects of used composite material on the temperature distribution of spherical shell are evaluated. Herein, the integral transform method is used to vanish the cross derivative term in heat transfer partial differential equation. The transferred equation is solved and two linearly-independent solutions for homogenous equation are found. Finally, using the Green's function theorem to find the particular solution of transferred heat equation and then applying an inverse transformation, the analytical solution is obtained.

2. GOVERNING EQUATIONS

Evaluating the balance of energy within differential element of present spherical shell, one can derive the heat transfer partial differential equation. To do so, having knowledge of the heat conduction basics in anisotropic media is necessary. In 錯誤！找不到參照來源。, a composite spherical shell, in which the fiber angle (ψ) is considered as the angle between tangent lines to the sphere in fiber and θ directions, is depicted.

Assuming an arbitrary fiber angle, directional conductive properties of composite material may vary based on the value of fiber angle. For further information about the basics of heat conduction in composite media, especially composite spheres, the authors strongly recommend reference to the article written by Norouzi *et al.*[39] and the heat conduction book by Ozisik [42]. Herein, derivation process of the heat transfer equation is not brought in detail and only some important relations will be presented.

https://doi.org/10.1017/jmech.2018.54 Published online by Cambridge University Press

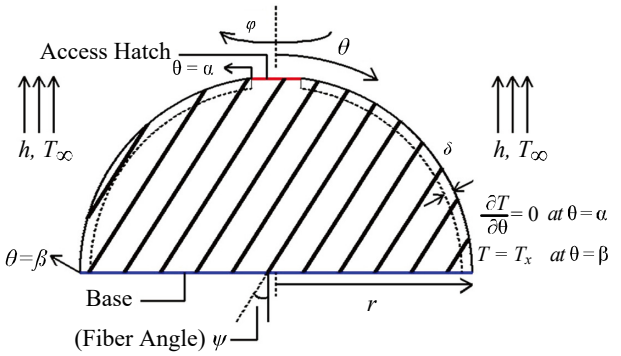


Fig. 1 Schematic geometry and boundary conditions of composite spherical vessel; the coordinate system is also shown.

Considering Fourier law as the fundamental heat conduction relation, equation (1) is presented for a composite spherical shell:

$$\begin{Bmatrix} q_\theta \\ q_\varphi \end{Bmatrix} = -\begin{bmatrix} k_{\theta\theta} & k_{\theta\varphi} \\ k_{\varphi\theta} & k_{\varphi\varphi} \end{bmatrix} \begin{Bmatrix} \dfrac{\partial T}{r\,\partial\theta} \\ \dfrac{\partial T}{r\sin(\theta)\,\partial\varphi} \end{Bmatrix} \tag{1}$$

In Eq. (1), r, θ and φ are spherical coordinate components where $0 \le \theta \le \pi$ and $0 \le \varphi \le 2\pi$ generally, q is heat flux and T is the temperature. In addition, the conduction coefficients in composite spherical shell, $k_{\theta\theta}$, $k_{\varphi\varphi}$ and $k_{\theta\varphi}$, are formulated using the conduction coefficient in fiber direction, k_{11}, perpendicular to the fiber direction k_{22}, and also the fiber angle value. It is noteworthy to mention that in present study, the heat conduction in a spherical composite shell is investigated. Consequently, the temperature gradients in radial direction are neglected.

$$k_{\theta\theta} = m_i^{\,2} k_{11} + n_i^{\,2} k_{22} \tag{2a}$$

$$k_{\varphi\varphi} = n_l^{\,2} k_{11} + m_l^{\,2} k_{22} \tag{2b}$$

$$k_{\theta\varphi} = k_{\varphi\theta} = m_l n_l (k_{11} - k_{22}) \tag{2b}$$

where m_l and n_l are equal to $\cos\psi$ and $\sin\psi$, respectively.

Herein, to take into account the effects of heat convection with ambient flow, external heat radiation, and also the possible heat generation within the spherical shell on temperature distribution, these factors are modeled in the heat transfer equation. To this end, balance of energy within a spherical element is applied. Finally, the equation of heat transfer in a composite spherical shell with the consideration of heat convection, external heat radiation, and possible heat generation is obtained as:

$$\frac{k_{\theta\theta}}{r^2\sin(\theta)}\left(\cos(\theta)\frac{\partial T}{\partial\theta} + \sin(\theta)\frac{\partial^2 T}{\partial\theta^2}\right) + \frac{k_{\varphi\varphi}}{r^2\sin(\theta)^2}\frac{\partial^2 T}{\partial\varphi^2} + \frac{2k_{\theta\varphi}}{r^2\sin(\theta)}\frac{\partial^2 T}{\partial\theta\,\partial\varphi} - \frac{h(T-T_\infty)}{\delta} = -\frac{q'' + g\delta}{\delta} \tag{3}$$

where h is the convection coefficient, q'' is an external heat radiation flux, g represents the heat generation rate per volume and δ is the thickness of spherical shell. Defining a modified temperature as $\Theta = T - T_\infty$, Eq. (3) is rewritten to a simpler form:

$$\frac{k_{\theta\theta}}{r^2\sin(\theta)}\left(\cos(\theta)\frac{\partial \Theta}{\partial\theta} + \sin(\theta)\frac{\partial^2 \Theta}{\partial\theta^2}\right) + \frac{k_{\varphi\varphi}}{r^2\sin(\theta)^2}\frac{\partial^2 \Theta}{\partial\varphi^2} + \frac{2k_{\theta\varphi}}{r^2\sin(\theta)}\frac{\partial^2 \Theta}{\partial\theta\,\partial\varphi} - \frac{h\Theta}{\delta} = -\frac{q'' + g\delta}{\delta} \tag{4}$$

In this solution, two boundaries located at $\theta_{b1} = \alpha$ and $\theta_{b2} = \beta$ are considered for the composite spherical shell. The general boundary conditions are dedicated at these boundaries as below:

$$\sigma_1 \Theta + \omega_1 \frac{\partial \Theta}{\partial\theta} = f_1(\varphi) \qquad \text{at } \theta_{b1} = \alpha \tag{5a}$$

$$\sigma_2 \Theta + \omega_2 \frac{\partial \Theta}{\partial\theta} = f_2(\varphi) \qquad \text{at } \theta_{b2} = \beta \tag{5b}$$

where $\sigma_1, \sigma_2, \omega_1$ and ω_2 are constant coefficients and f_1 and f_2 can be any arbitrary functions of variable φ.

In present solution, g has a constant value regardless of the spatial position. In addition, different environmental conditions can be applied to the composite spherical shell based on the desired application. As a result, the external heat flux, q'', can be defined based on the specified application of the spherical shell. Details about the heat flux distribution will be addressed in the Results section.

3. METHOD OF SOLUTION

To solve the differential equations like Eq. (4), one of methods usually used, is the separation of variables method. However, due to existence of a cross derivative term in the Eq. (4), which is because of the anisotropy in composite materials (effect of variable fiber angle), applying the separation of variables method directly on Eq. (4), is not beneficial. The first step to solve equation (4), is to avoid this cross derivative term. To this end, the integral transform method is used and Eq. (4) is transformed, with respect to φ, to a new equation in which the cross derivative term vanishes. The integral transform with respect to φ is defined as:

https://doi.org/10.1017/jmech.2018.54 Published online by Cambridge University Press

$$\hat{\Theta}(\theta,n)=\int_{-\pi}^{\pi}e^{-in\varphi'}\Theta(\theta,\varphi')\,d\varphi', \tag{6a}$$

$$\Theta(\theta,\varphi)=\frac{1}{2\pi}\sum_{n=-\infty}^{\infty}e^{in\varphi}\hat{\Theta}(\theta,n), \tag{6b}$$

where $i^2=-1$ and the integer n is the transform variable.

Applying the integral transform on the Eq. (4), generates an ordinary differential equation:

$$\frac{d^2\hat{\Theta}}{d\theta^2}+\left(\frac{2ink_{\theta\varphi}}{k_{\theta\theta}\sin(\theta)}+\cot(\theta)\right)\frac{d\hat{\Theta}}{d\theta}-\left(\frac{hr^2}{\delta k_{\theta\theta}}+\frac{n^2k_{\varphi\varphi}}{k_{\theta\theta}\sin(\theta)^2}\right)\hat{\Theta}=-\frac{r^2(\hat{q}''+g\delta)}{\delta k_{\theta\theta}} \tag{7}$$

where $\hat{q}''$ is integral transform of the external heat radiation flux (q'').

According to the theory of ordinary differential equations, general solution of Eq. (7) is as follows [43]:

$$\hat{\Theta}(\theta,n)=C_1\hat{\Theta}_1(\theta,n)+C_2\hat{\Theta}_2(\theta,n)+\hat{\Theta}_p(\theta,n) \tag{8}$$

where C_1 and C_2 are two arbitrary constants, $\hat{\Theta}(\theta,n)=\hat{\Theta}_1(\theta,n)$ and $\hat{\Theta}(\theta,n)=\hat{\Theta}_2(\theta,n)$ are two linearly independent solutions of the homogeneous form of Eq. (7), and $\hat{\Theta}_p(\theta,n)$ is a particular solution for Eq. (7) [43]. The mentioned linearly independent solutions for homogeneous form of Eq. (7) are:

$$\hat{\Theta}_1(\theta,n)=(\cos(\theta)-1)^{-\frac{a+1}{4}}(\cos(\theta)+1)^{\frac{a-1}{4}}\left(\frac{\cos(\theta)-1}{2}\right)^{\frac{1}{2}+\frac{1}{4}\sqrt{a^2-2a+4b+1}}\left(\frac{\cos(\theta)+1}{2}\right)^{\frac{1}{2}-\frac{1}{4}\sqrt{a^2+2a+4b+1}}F_1 \tag{9a}$$

$$\hat{\Theta}_2(\theta,n)=(\cos(\theta)-1)^{-\frac{a+1}{4}}(\cos(\theta)+1)^{\frac{a-1}{4}}\left(\frac{\cos(\theta)-1}{2}\right)^{\frac{1}{2}+\frac{1}{4}\sqrt{a^2-2a+4b+1}}\left(\frac{\cos(\theta)+1}{2}\right)^{\frac{1}{2}+\frac{1}{4}\sqrt{a^2+2a+4b+1}}F_2 \tag{9b}$$

where the functions F_1 and F_2 are defined as:

$$F_1=\text{Hypergeom}\left(\begin{bmatrix}\frac{1}{4}\sqrt{a^2-2a+4b+1}+i\sqrt{c}-\frac{1}{4}\sqrt{a^2+2a+4b+1}+\frac{1}{2},\\ \frac{1}{4}\sqrt{a^2-2a+4b+1}-i\sqrt{c}-\frac{1}{4}\sqrt{a^2+2a+4b+1}+\frac{1}{2}\end{bmatrix};1-\frac{1}{2}\sqrt{a^2+2a+4b+1};\frac{\cos(\theta)+1}{2}\right) \tag{10a}$$

$$F_2=\text{Hypergeom}\left(\begin{bmatrix}\frac{1}{4}\sqrt{a^2-2a+4b+1}+i\sqrt{c}+\frac{1}{4}\sqrt{a^2+2a+4b+1}+\frac{1}{2},\\ \frac{1}{4}\sqrt{a^2-2a+4b+1}-i\sqrt{c}+\frac{1}{4}\sqrt{a^2+2a+4b+1}+\frac{1}{2}\end{bmatrix};1+\frac{1}{2}\sqrt{a^2+2a+4b+1};\frac{\cos(\theta)+1}{2}\right) \tag{10b}$$

In addition, in Eqs. (9) and (10), the parameters *a*, *b* and *c* are defined as:

$$a=\frac{2ink_{\theta\varphi}}{k_{\theta\theta}} \tag{11a}$$

$$b=\frac{n^2k_{\varphi\varphi}}{k_{\theta\theta}} \tag{11b}$$

$$c=\frac{hr^2}{\delta k_{\theta\theta}} \tag{11c}$$

https://doi.org/10.1017/jmech.2018.54 Published online by Cambridge University Press

In Eqs. (10a) and (10b), the term *Hypergeom* refers to hypergeometric function, which is a special function represented by hypergeometric series, possesses various special functions as specific cases [44]. The mathematical definition of hypergeometric function, which is a solution of a second order linear ordinary differential equation, is comprehensively brought in several relevant textbooks. For further information, the authors recommend reference to the handbook written by Abramowitz and Stegun [44].

To obtain the particular solution for Eq. (7) ($\hat{\Theta}_p(\theta,n)$), the Green's function theorem is used [43]. However, before calculating the particular solution using Green's function, the Sturm-Liouville form of Eq. (7) must be defined [43]. The Sturm-Liouville form of Eq. (7) is as follows [43]:

$$\frac{d}{d\theta}\left(p\frac{d\hat{\Theta}}{d\theta}\right)+(j+\lambda s)\hat{\Theta}=-f \tag{12}$$

where the unknown coefficients in Eq. (12), using the coefficients in Eq. (7), are defined as [43]:

$$p(\theta)=\exp\left[\int^{\theta}\left(\frac{2ink_{\theta\varphi}}{k_{\theta\theta}\sin(t)}+\cot(t)\right)dt\right] \tag{13a}$$

$$j(\theta)=-\frac{n^2k_{\varphi\varphi}}{k_{\theta\theta}\sin(\theta)^2}p(\theta) \tag{13b}$$

$$s(\theta)=p(\theta) \tag{13c}$$

$$f(\theta)=\frac{r^2(\hat{q}''+g\delta)}{\delta k_{\theta\theta}}p(\theta) \tag{13d}$$

$$\lambda=-\frac{hr^2}{\delta k_{\theta\theta}} \tag{13d}$$

Therefore, the particular solution based on the Green's function theorem is calculated as [43]:

$$\hat{\Theta}_p(\theta,n)=-\int_{\alpha}^{\theta}\frac{\hat{\Theta}_2(\theta,n)\,\hat{\Theta}_1(\xi,n)}{p(\xi)\,W(\xi)}f(\xi)\,d\xi-\int_{\theta}^{\beta}\frac{\hat{\Theta}_1(\theta,n)\,\hat{\Theta}_2(\xi,n)}{p(\xi)\,W(\xi)}f(\xi)\,d\xi \tag{14}$$

where $W=(\hat{\Theta}_1\Theta_2'-\hat{\Theta}_2\Theta_1')$ is non-zero Wronskian of the solutions $\hat{\Theta}_1$ and $\hat{\Theta}_2$. Substituting Eqs. (9) and (14) into the Eq. (8), the general solution of Eq. (7) is achieved. However, to obtain the general solution of Eq. (4), it is required to transform Eq. (8) using the inverse integral transform shown in Eq. (6b). Consequently, the general solution of Eq. (4) is calculated as:

$$\Theta(\theta,\varphi)=\frac{1}{2\pi}\sum_{n=-\infty}^{\infty}e^{in\varphi}\left(C_1\hat{\Theta}_1(\theta,n)+C_2\hat{\Theta}_2(\theta,n)+\hat{\Theta}_p(\theta,n)\right) \tag{15}$$

In Eq. (15), the unknown coefficients C_1 and C_2 are calculable considering the general boundary conditions on the boundaries located at $\theta_{b1}=\alpha$ and $\theta_{b2}=\beta$. Therefore, after substituting the general solution in Eq. (15) into Eqs. (5a) and (5b), following equations are achieved:

$$\frac{1}{2\pi}\sum_{n=-\infty}^{\infty}e^{in\varphi}\begin{bmatrix}\sigma_1\left(C_1\hat{\Theta}_1(\alpha,n)+C_2\hat{\Theta}_2(\alpha,n)+\hat{\Theta}_p(\alpha,n)\right)+\\ \omega_1\left(C_1\hat{\Theta}_1'(\alpha,n)+C_2\hat{\Theta}_2'(\alpha,n)+\hat{\Theta}_p'(\alpha,n)\right)\end{bmatrix}=f_1(\varphi) \tag{16a}$$

$$\frac{1}{2\pi}\sum_{n=-\infty}^{\infty}e^{in\varphi}\begin{bmatrix}\sigma_2\left(C_1\hat{\Theta}_1(\beta,n)+C_2\hat{\Theta}_2(\beta,n)+\hat{\Theta}_p(\beta,n)\right)+\\ \omega_2\left(C_1\hat{\Theta}_1'(\beta,n)+C_2\hat{\Theta}_2'(\beta,n)+\hat{\Theta}_p'(\beta,n)\right)\end{bmatrix}=f_2(\varphi) \tag{16b}$$

where the prime sign denotes derivation with respect to θ. Now, the complex Fourier series of functions f_1 and f_2 are obtained as:

https://doi.org/10.1017/jmech.2018.54 Published online by Cambridge University Press

$$f_1(\varphi)=\frac{1}{2\pi}\sum_{n=-\infty}^{\infty}\kappa_{1n}\,e^{in\varphi} \tag{17a}$$

$$f_2(\varphi)=\frac{1}{2\pi}\sum_{n=-\infty}^{\infty}\kappa_{2n}\,e^{in\varphi} \tag{17b}$$

Finally, the unknown coefficients C_1 and C_2 are calculated using Eqs. (16) and (17):

$$C_1=C_{1n}=\frac{\left(\kappa_{1n}-\begin{pmatrix}\sigma_1\hat{\Theta}_p(\alpha,n)+\\ \omega_1\hat{\Theta}'_p(\alpha,n)\end{pmatrix}\right)\begin{pmatrix}\sigma_1\hat{\Theta}_2(\beta,n)+\\ \omega_1\hat{\Theta}'_2(\beta,n)\end{pmatrix}-\left(\kappa_{2n}-\begin{pmatrix}\sigma_1\hat{\Theta}_p(\beta,n)+\\ \omega_1\hat{\Theta}'_p(\beta,n)\end{pmatrix}\right)\begin{pmatrix}\sigma_1\hat{\Theta}_2(\alpha,n)+\\ \omega_1\hat{\Theta}'_2(\alpha,n)\end{pmatrix}}{\begin{pmatrix}\sigma_1\hat{\Theta}_1(\alpha,n)+\\ \omega_1\hat{\Theta}'_1(\alpha,n)\end{pmatrix}\begin{pmatrix}\sigma_1\hat{\Theta}_2(\beta,n)+\\ \omega_1\hat{\Theta}'_2(\beta,n)\end{pmatrix}-\begin{pmatrix}\sigma_1\hat{\Theta}_1(\beta,n)+\\ \omega_1\hat{\Theta}'_1(\beta,n)\end{pmatrix}\begin{pmatrix}\sigma_1\hat{\Theta}_2(\alpha,n)+\\ \omega_1\hat{\Theta}'_2(\alpha,n)\end{pmatrix}} \tag{18a}$$

$$C_2=C_{2n}=\frac{\left(\kappa_{2n}-\begin{pmatrix}\sigma_1\hat{\Theta}_p(\beta,n)+\\ \omega_1\hat{\Theta}'_p(\beta,n)\end{pmatrix}\right)\begin{pmatrix}\sigma_1\hat{\Theta}_1(\alpha,n)+\\ \omega_1\hat{\Theta}'_1(\alpha,n)\end{pmatrix}-\left(\kappa_{1n}-\begin{pmatrix}\sigma_1\hat{\Theta}_p(\alpha,n)+\\ \omega_1\hat{\Theta}'_p(\alpha,n)\end{pmatrix}\right)\begin{pmatrix}\sigma_1\hat{\Theta}_1(\beta,n)+\\ \omega_1\hat{\Theta}'_1(\beta,n)\end{pmatrix}}{\begin{pmatrix}\sigma_1\hat{\Theta}_1(\alpha,n)+\\ \omega_1\hat{\Theta}'_1(\alpha,n)\end{pmatrix}\begin{pmatrix}\sigma_1\hat{\Theta}_2(\beta,n)+\\ \omega_1\hat{\Theta}'_2(\beta,n)\end{pmatrix}-\begin{pmatrix}\sigma_1\hat{\Theta}_1(\beta,n)+\\ \omega_1\hat{\Theta}'_1(\beta,n)\end{pmatrix}\begin{pmatrix}\sigma_1\hat{\Theta}_2(\alpha,n)+\\ \omega_1\hat{\Theta}'_2(\alpha,n)\end{pmatrix}} \tag{18b}$$

4. RESULTS AND DISCUSSION

4.1 Application of composite spherical shells

Composite spherical shells are used in variety of industrial applications. A case in point is the spherical pressure vessels [45, 46]. Pressure vessels are used in mining operations, oil refineries and petrochemical plants, pneumatic and hydraulic reservoir, submarine and space ship habitats, and storage vessels [45]. Particularly, spherical pressure vessels are frequently used as high pressure storage tanks for liquid natural gas, liquid petroleum gas, butane, propane, ammonia, oxygen, hydrogen and nitrogen [45]. Although pressure vessels are usually made of steel, some of which are produced by composite materials such as filament wound composite [45, 46].

In present study, the composite spherical shell is considered as a spherical pressure vessel containing an arbitrary high pressurized liquid gas such as liquid natural gas. For present spherical pressure vessel, one access hatch located at the top of that ($0\le\theta<\alpha$) is considered. In addition, it is assumed that the base of present spherical vessel sits on the ground at $\theta=\beta$.

4.2 Modeling the environmental conditions

Sun radiation on the pressure vessels, is one of major external environmental factors affecting the temperature of both pressure vessel and the reserved fluid. The increase in temperature of reserved fluid makes an increase in internal pressure of vessel. Moreover, increase in the temperature of pressure vessel may increase the possibility of crack and rupture formation on its surface. Totally, both of current events are dangerous and important to be considered in design process in order to prevent explosion of such huge structures. In present solution, sun radiation is defined as:

$$q''=\begin{cases}\dfrac{q_0}{2}\left(\cos(\theta/2)+\sin(\varphi)\right) & 0\le\varphi\le\pi\\ \dfrac{q_0}{2}\cos(\theta/2) & \pi<\varphi<2\pi\end{cases} \tag{19}$$

where q_0 is average of sun heat flux on the earth and is equal to 1357 W/m2 [47]. In addition, it is considered that the spherical pressure vessel is cooled by air. Table 1 is provided to introduce the properties of graphite/epoxy composite material which is a common used material for pressure vessels [45].

Table 1 Properties of graphite/epoxy composite materials [49].

k in parallel direction of fibers (k_{11})	11.1 W/mK
k in perpendicular direction of fibers (k_{22})	0.87 W/mK
Volumetric percentage of fibers	75
Melting point	450 K
Heat capacity	935 J/kgK
Density	1400 kg/m^3

The properties of composite materials are severely affected by factors including raw materials, manufacturing processes, and additional treatments, and

https://doi.org/10.1017/jmech.2018.54 Published online by Cambridge University Press

so on [48]. Consequently, in order to investigate the effects of conductivity coefficients on temperature distribution, it is considered that the k_{11}/k_{22} ratio of graphite/epoxy can possess variety of values. Therefore, Table 2 is presented by which three other materials, in addition to graphite/epoxy, are defined in a way that their difference is only in the value of heat conductivity coefficient in fiber direction (k_{11}).

Table 2 Heat conductivity properties of four defined materials.

Material number	$k_{11}\ (W/mK)$	$k_{22}\ (W/mK)$	$K_r = k_{11}/k_{22}$
1	0.87	0.87	1
2 (graphite/epoxy)	11.1	0.87	12.76
3	87	0.87	100
4	174	0.87	200

According to Table 2, material 1 is homogenous, material 2 is graphite/epoxy and materials 3 and 4 are two highly anisotropic ones. Table 3 includes geometry and boundary conditions of present composite spherical vessel.

Table 3 Geometry and boundary conditions of composite spherical vessel.

Radius (r)	1 m
Thickness of spherical shell (δ)	0.01 m
Boundary of the access hatch (α)	5 degrees
Boundary of the base (β)	90 degrees
Convection coefficient (h)	20 $W/m^2 K$
Average of sun heat flux (q_0)	1357 W/m^2
σ_1 , σ_2	0, 1
ω_1 , ω_2	1, 0
f_1	0
f_2	0
T_∞	300 K

4.3 Validation of analytical solution

Present analytical solution is verified by numerical calculation of heat conduction equation based on a second order finite difference scheme. In Fig. 2 , two plots are drawn by which the analytical distribution and numerical solution of temperature are shown using solid lines and markers, respectively. The temperature variations are depicted for four values of fiber angle in both θ and φ directions which the composite material is graphite/epoxy (material 2). Fig. 2 shows an excellent agreement between analytical and numerical solutions. In addition, distinct differences in the temperature distribution near boundaries, for different values of fiber angle, are observable in Fig. 2 -a. Besides, Fig. 2-b that illustrates the temperature variations at $\theta = 10°$ (close to the access hatch boundary), indicates such differences.

4.4 Other results

To present the temperature distribution on the surface of spherical vessel at different fiber angle values, Fig. 2 is depicted. In this figure, the composite material is graphite/epoxy (material 2) and the temperature distribution on front side and back side of the sphere are displayed. As shown, with increase in fiber angle value, effects of the boundary conditions on the interior domain is declined. It is mainly attributed to the bigger value of conductivity coefficient in fiber direction in comparison with the other orthogonal direction. In addition, size and location of the region showing big values of temperature, differ at each fiber angle. At $\psi = 0^\circ$, the location of

https://doi.org/10.1017/jmech.2018.54 Published online by Cambridge University Press

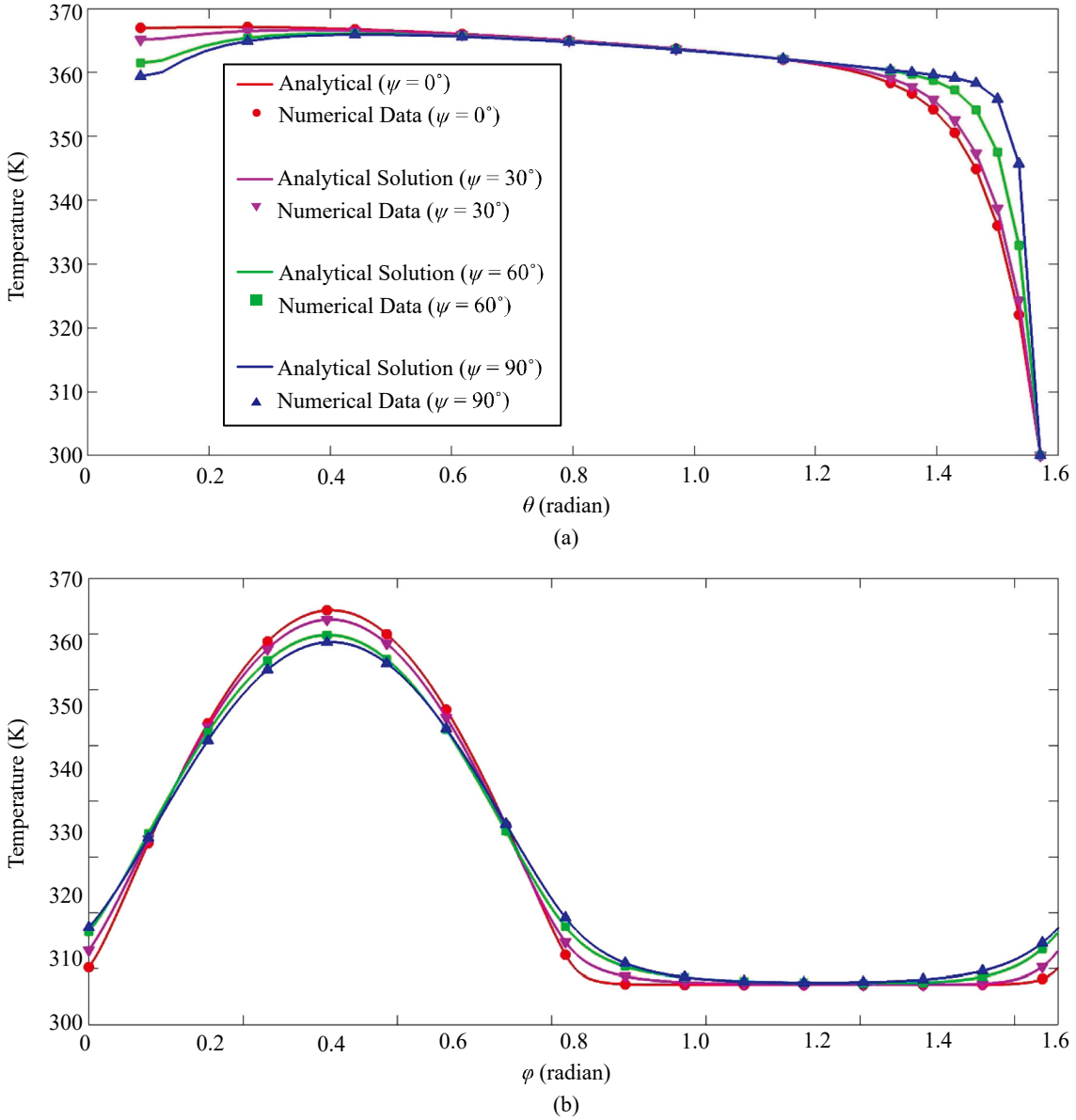


Fig. 2 Validation of present analytical results with numerical solution for different values of fiber angle which the composite material is graphite/epoxy (material 2); a) temperature variations in θ direction at $\varphi = 90^\circ$, b) temperature variations in φ direction at $\theta = 10^\circ$

region with high temperature is close to the upper boundary, however, with increase in the fiber angle, it moves towards the interior domain.

Current results are more visible for Fig. 3 in which the composite material is material 3 possessing a high value for k_{11}/k_{22}. An interesting point extracted from Fig. 3 is the maximum temperature value which seems to be reduced with increase in fiber angle value. The reason behind that might be the increase in the value of conductivity coefficient in φ direction which increases the rate of heat conduction towards back side of the vessel leading to reduction in the value of maximum temperature. In addition, a deviated orientation of temperature with respect to θ direction at $\psi = 30°$ and $\psi = 60°$ is observable. This deviation is more severe in Fig. 3 compared to Fig. 3, in which the value of k_{11}/k_{22} is bigger.

In Fig. 5, similar contours to those of Fig. 2 and Fig. 3 are depicted. However, the trends discussed for Fig. 2 and Fig. 3, are intensified in Fig. 4 in which the ratio of k_{11}/k_{22} is twice the ratio used in Fig. 3.

In Fig. 5, the mean temperature in φ direction versus θ direction is depicted for mentioned quadruple materials at four different values of fiber angle. This figure shows a clear distinction between temperature variations for the used materials so that with increase in the fiber angle value, the values of mean temperature for materials 2-4 move towards the mean temperature distribution of the homogenous material (material 1). In addition, Fig. 6 implies that for major values of fiber angle, the higher ratio of k_{11}/k_{22}, generates lower mean temperature on

https://doi.org/10.1017/jmech.2018.54 Published online by Cambridge University Press

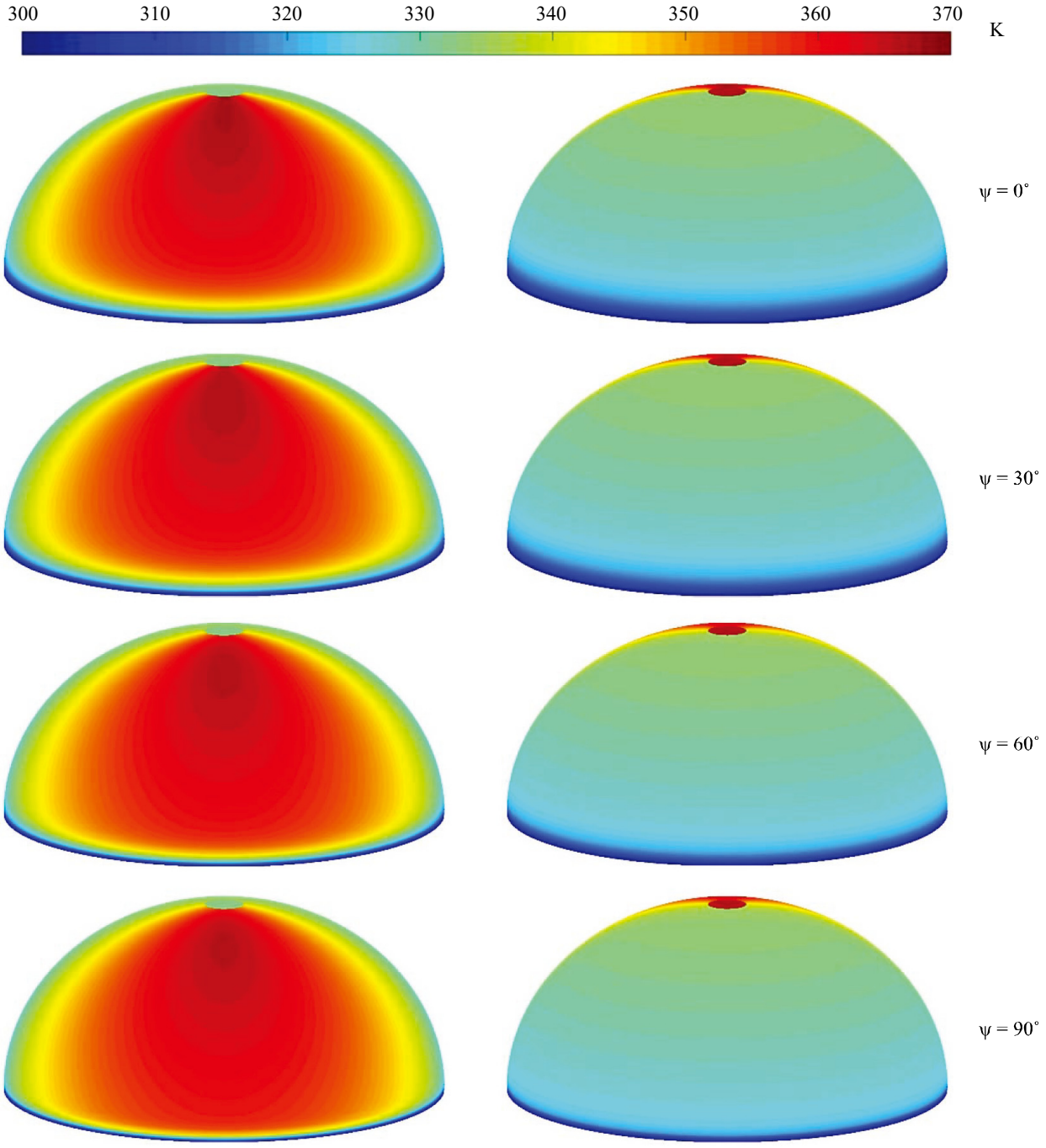


Fig. 2 Temperature contours of composite spherical vessel for four fiber angles which the composite material is material 2; a) front side, b) back side

the surface of spherical vessel. Besides, this figure confirms the fact mentioned before about the increased effects of boundary conditions for smaller value of fiber angle and higher ratio of k_{11}/k_{22}.

Fig. 6 presents the mean temperature in θ direction versus φ direction for materials 1-4 at four different values of fiber angle. This figure shows a general lower temperature distribution for higher ratio of k_{11}/k_{22} at $\psi = 0^\circ$ and $\psi = 30^\circ$; however, at $\psi = 60^\circ$ and $\psi = 90^\circ$, a similar trend doesn't exist. With increase in fiber angle value for materials 2-4, the conductivity coefficient in φ direction increases leading to raised heat conduction towards back side of the vessel. In addition, with increase in fiber angle value, the effects of boundary conditions on the temperature distribution decreases (due to reduced value of conductivity coefficient in θ direction), which generates generally grown temperature values for each individual composite material.

https://doi.org/10.1017/jmech.2018.54 Published online by Cambridge University Press

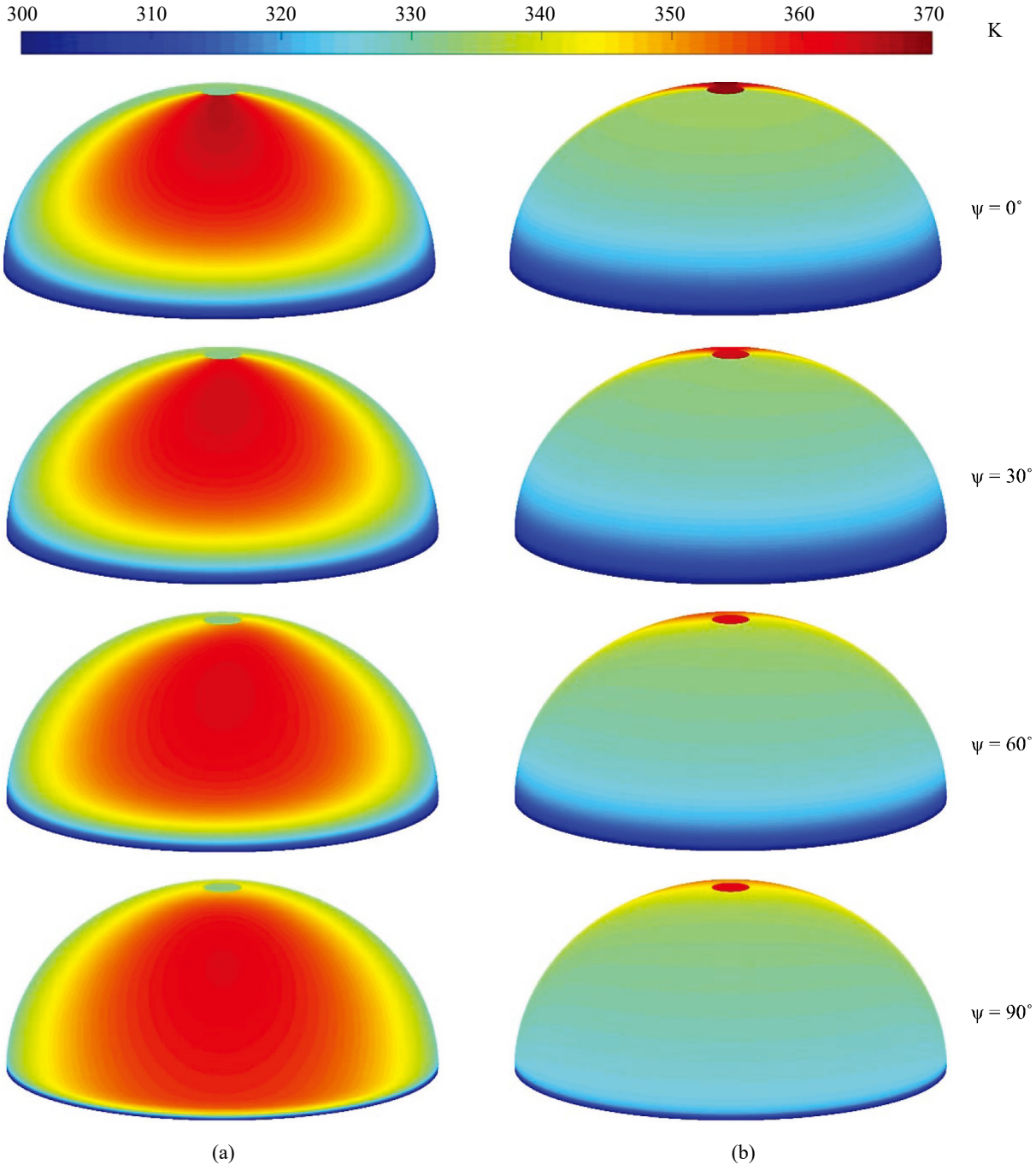


Fig. 3 Temperature contours of composite spherical vessel for four fiber angles which the composite material is material 3; a) front side, b) back side.

Fig 8 is presented in order to show the mean temperature of the composite spherical vessel versus different values of fiber angle for materials 2-4. This figure shows that for major values of fiber angle, the material 4, which possesses the biggest value for conductivity coefficient in fiber direction (k_{11}) compared to other materials, indicates lowest values for mean temperature of the composite spherical vessel. Generally, a lower fiber angle value generates lower value of mean temperature for all used materials. However, the most interesting finding is the equivalence of mean temperatures of materials 2-4 at $\psi = 90^{\circ}$. Based on the objective of having the lowest mean temperature, this figure proposes the fiber angle equal to zero as the most efficient value for all used materials.

In Fig. 8, maximum temperature of the composite spherical vessel versus different values of fiber angle for materials 2-4 is depicted. Similar to the results extracted from Fig. 7, in Fig. 8, the maximum temperature is generally the lowest for material 4 which has the biggest value of conductivity coefficient in fiber direction. Fig. 8 shows that the lowest value of maximum temperature for

https://doi.org/10.1017/jmech.2018.54 Published online by Cambridge University Press

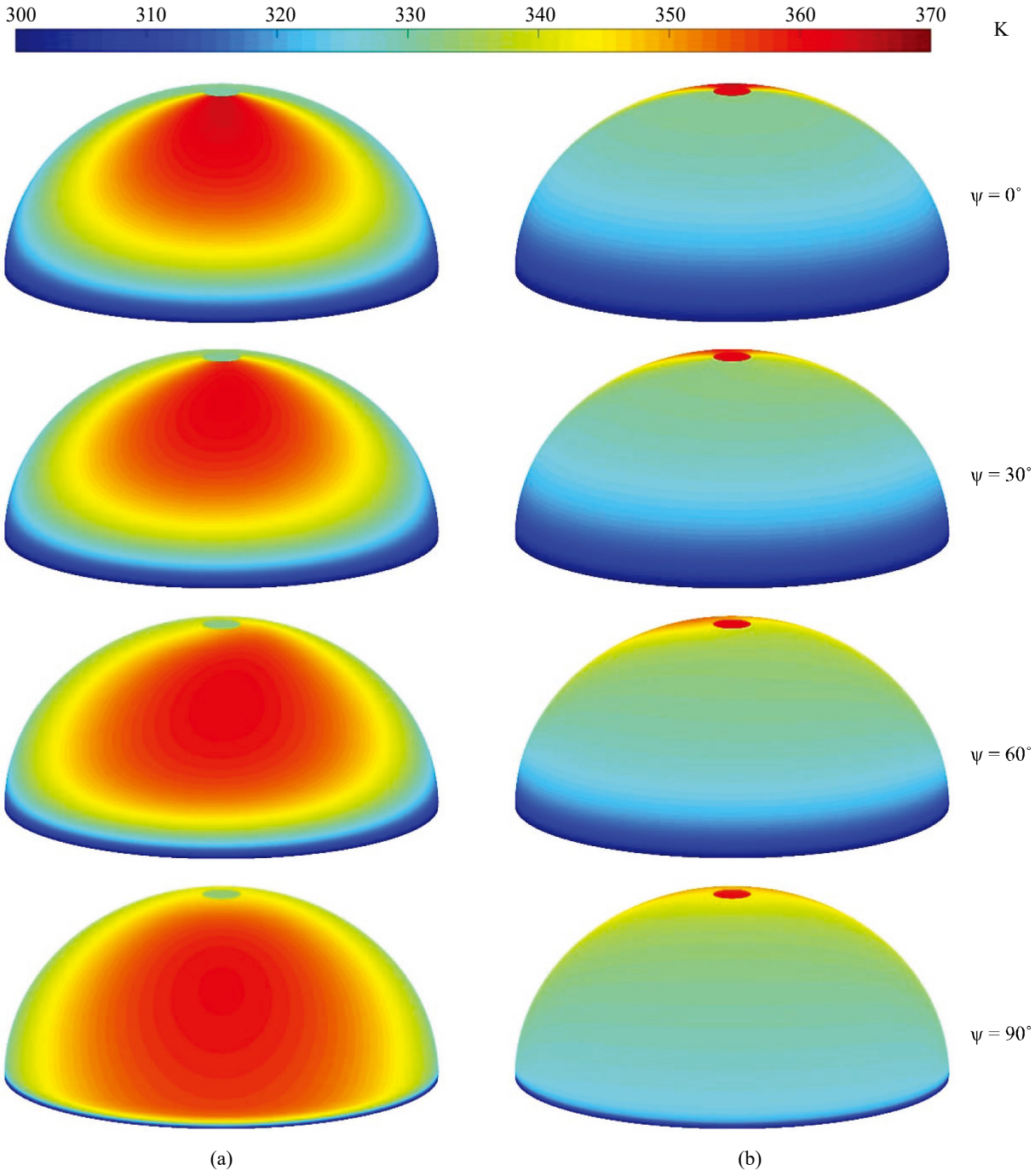


Fig. 4 Temperature contours of composite spherical vessel for four fiber angles which the composite material is material 4; a) front side, b) back side.

each material occurs at $\psi = 90^{\circ}$. Consequently, based on consideration of the maximum temperature as the main design parameter, this figure proposes the fiber angle value equal to 90 degrees as the most efficient choice. Current finding contradicts with the proposal of Fig. 7.

To sum up, in present study, it is proposed to consider both the mean and maximum temperature of composite spherical vessel as the design factors. Maximum temperature is important because it creates a region with high temperature leading to a big value for local thermal stress on the composite vessel. In addition, the mean temperature is also important because it affects the thermal stresses and the pressure of the reserved fluid in a wide range. Thus, herein, the authors propose to define a target function containing both maximum and mean temperature as its parameters and then select the most efficient value for fiber angle based on that

https://doi.org/10.1017/jmech.2018.54 Published online by Cambridge University Press

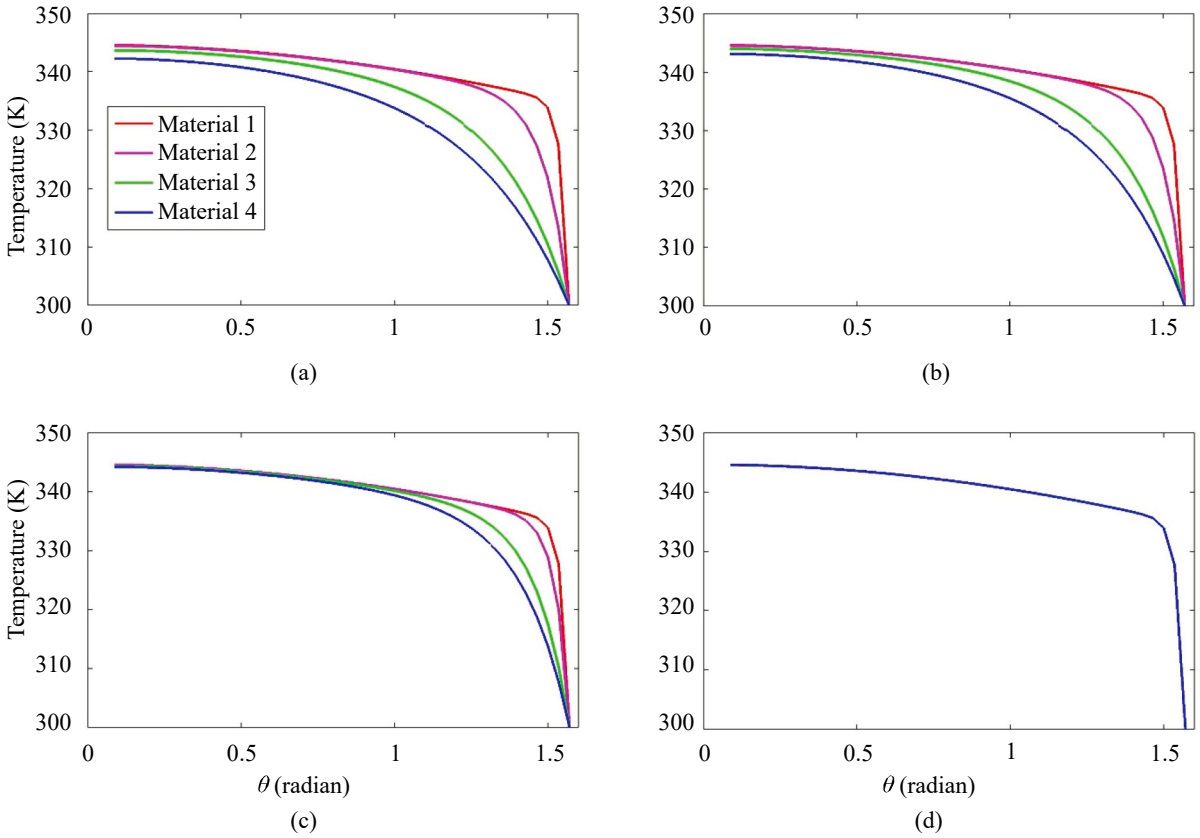


Fig. 5 Mean temperature in φ direction versus θ direction for materials 1-4; a) $\psi = 0^\circ$, b) $\psi = 30^\circ$, c) $\psi = 60^\circ$, d) $\psi = 90^\circ$

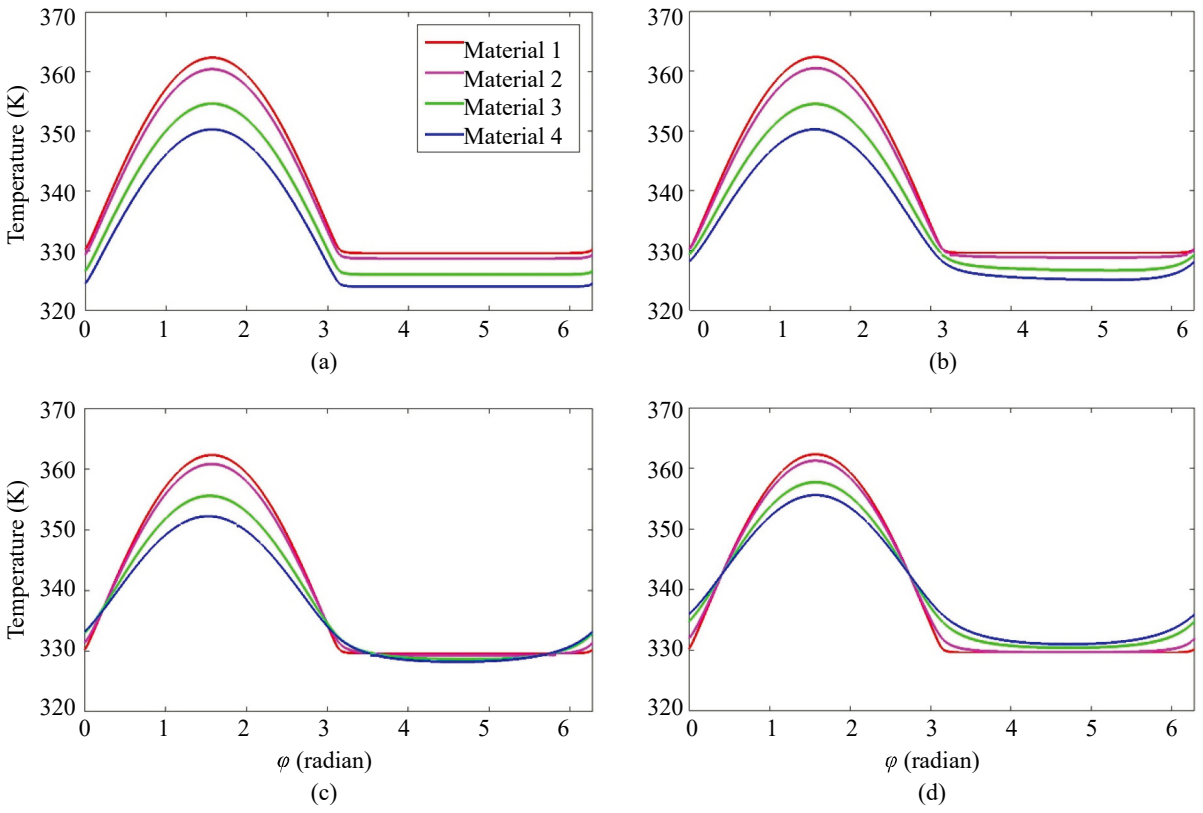


Fig. 6 Mean temperature in θ direction versus φ direction for materials 1-4; a) $\psi = 0^\circ$, b) $\psi = 30^\circ$, c) $\psi = 60^\circ$, d) $\psi = 90^\circ$

https://doi.org/10.1017/jmech.2018.54 Published online by Cambridge University Press

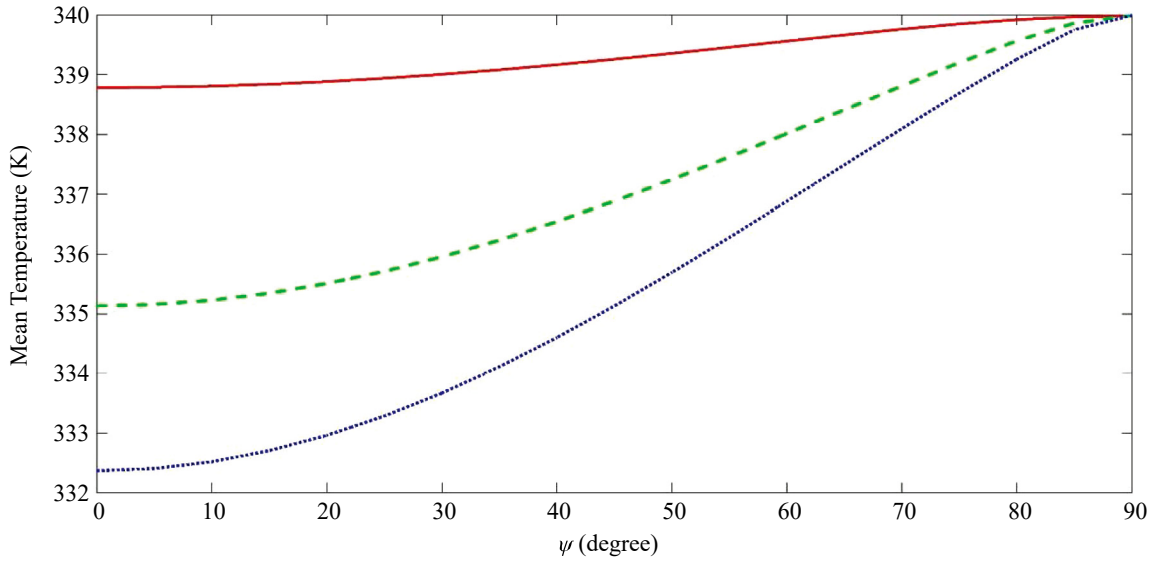


Fig. 7 Mean temperature of composite spherical vessel versus fiber angle for materials 2-4; solid line (red): material 2 (graphite/epoxy), dashed line (green): material 3, dotted line (blue): material 4.

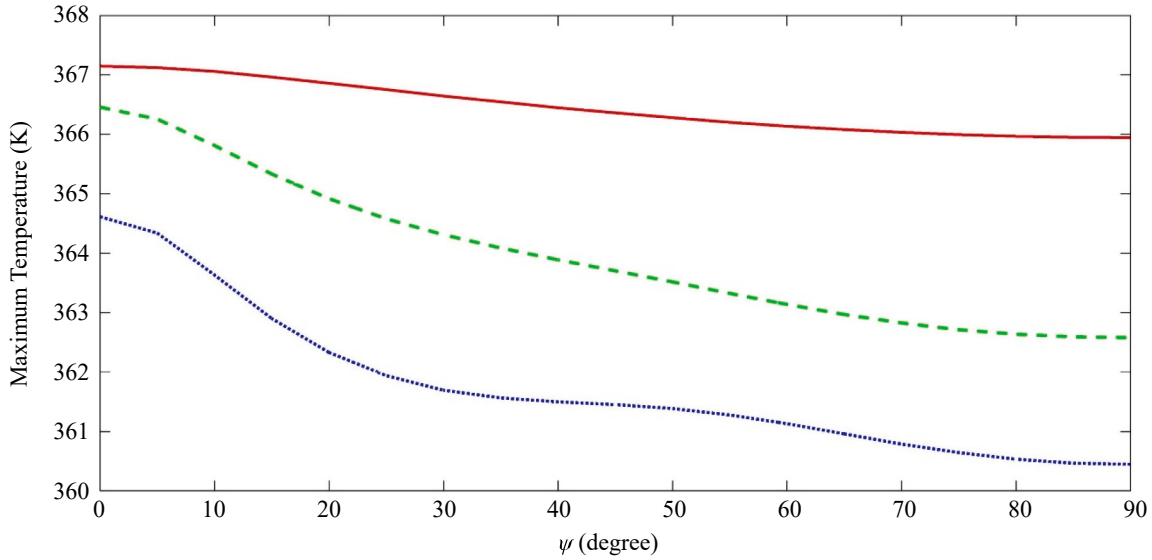


Fig. 8 Maximum temperature of composite spherical vessel versus fiber angle for materials 2-4; solid line (red): material 2 (graphite/epoxy), dashed line (green): material 3, dotted line (blue): material 4.

5. CONCLUSIONS

In the present paper, an analytical solution was obtained for the problem of anisotropic heat conduction in truncated composite spherical shells. Particularly, the steady-state solution was developed to find the temperature distribution in a composite spherical vessel. Defining four materials differing in the value of conductivity coefficient in fiber direction, the effects of used composite material on the temperature distribution were evaluated. In addition, different values of fiber angle were checked to analyze the effects of fiber angle on the temperature distribution. The figure showing mean temperature of composite vessel versus fiber angle values proposed the zero value for fiber angle as the most efficient choice, however, the value of 90 degrees was proposed by another figure showing the maximum temperature versus fiber angle. Therefore, herein, the authors propose to objectively consider the mean and maximum temperature of composite spherical vessel as design factors to choose the most efficient value of fiber angle. To this end, definition of a target function containing both mean and maximum temperatures as its parameters seems necessary.

For future works, the authors propose study on the transient anisotropic heat conduction in a truncated composite spherical shell, analytically

https://doi.org/10.1017/jmech.2018.54 Published online by Cambridge University Press

KNOWLEGMENTS

The authors declare that they have no conflict of interest with anybody or any institute

REFERENCES

1. Barrett, D.J., "The mechanics of z-fiber reinforcement," *Composite Structures*, **312**, pp. 23–32 (1996).
2. Mair, R.I., "Advanced composite structures research in Australia," *Composite Structures*, **57**, pp. 3–10 (2002).
3. Chao, C., Chen, F. and Shen, M., "An exact solution for thermal stresses in a three-phase composite cylinder under uniform heat flow," *International journal of solids and structures*, **44**, pp. 926–940 (2007).
4. Xiao, J., Gilhooley, D., Batra, R., Gillespie, J. and McCarthy, M., "Analysis of thick composite laminates using a higher-order shear and normal deformable plate theory (HOSNDPT) and a meshless method," *Composites Part B: Engineering*, **39**, pp. 414–427 (2008).
5. Pradeep, V. and Ganesan, N., "Thermal buckling and vibration behavior of multi-layer rectangular viscoelastic sandwich plates," *Journal of Sound and Vibration*, **310**, pp. 169–183 (2008).
6. Papargyris, D., Day, R., Nesbitt, A. and Bakavos, D., "Comparison of the mechanical and physical properties of a carbon fibre epoxy composite manufactured by resin transfer moulding using conventional and microwave heating," *Composites Science and Technology*, **68**, pp. 1854–1861 (2008).
7. Topal, U. and Uzman, Ü., "Thermal buckling load optimization of laminated composite plates," Thin-Walled Structures, **46**, pp. 667–675 (2008).
8. Antonucci, V., Giordano, M., Hsiao, K.T. and Advani, S.G., "A methodology to reduce thermal gradients due to the exothermic reactions in composites processing," *International journal of heat and mass transfer*, **45**, pp. 1675–1684 (2002).
9. Guo, Z.S., Du, S. and Zhang, B., "Temperature field of thick thermoset composite laminates during cure process," *Composites science and technology*, **65**, pp. 517–523 (2005).
10. Behzad, T. and Sain, M., "Finite element modeling of polymer curing in natural fiber reinforced composites," *Composites Science and Technology*, **67**, pp. 1666–1673 (2007).
11. Dlouhy, I., Chlup, Z., Boccaccini, D., Atiq, S. and Boccaccini, A., "Fracture behaviour of hybrid glass matrix composites: thermal ageing effects," *Composites Part A: Applied Science and Manufacturing*, **34**, pp. 1177–1185 (2003).
12. Gilbert, A., Kokini, K. and Sankarasubramanian, S., "Thermal fracture of zirconia–mullite composite thermal barrier coatings under thermal shock: An experimental study," *Surface and Coatings Technology*, **202**, pp. 2152–2161 (2008).
13. Gilbert, A., Kokini, K. and Sankarasubramanian, S., "Thermal fracture of zirconia–mullite composite thermal barrier coatings under thermal shock: A numerical study," *Surface and Coatings Technology*, **203**, pp. 91–98 (2008).
14. Wang, F., Hua, Q. and Liu, C.S., "Boundary function method for inverse geometry problem in two-dimensional anisotropic heat conduction equation," *Applied Mathematics Letters*, **84**, pp. 130-136 (2018).
15. Gu, Y., He, X., Chen, W. and Zhang, C., "Analysis of three-dimensional anisotropic heat conduction problems on thin domains using an advanced boundary element method," *Computers & Mathematics with Applications*, **75(1)**, pp. 33-44 (2018).
16. Wang, F., Chen, W., Qu, W. and Gu, Y., "A BEM formulation in conjunction with parametric equation approach for three-dimensional Cauchy problems of steady heat conduction," *Engineering Analysis with Boundary Elements*, **63**, pp. 1-14 (2016).
17. Dülk, I. and Kovácsházy, T., "Steady-state heat conduction in multilayer bodies: An analytical solution and simplification of the eigenvalue problem," *International Journal of Heat and Mass Transfer*, **67**, pp. 784–797 (2013).
18. De Monte, F., "Transient heat conduction in one-dimensional composite slab. A 'natural'analytic approach," *International Journal of Heat and Mass Transfer*, **43**, pp. 3607–3619 (2000).
19. De Monte, F., "An analytic approach to the unsteady heat conduction processes in one-dimensional composite media," *International Journal of Heat and Mass Transfer*, **45**, pp. 1333–1343 (2002).
20. De Monte, F., "Unsteady heat conduction in two-dimensional two slab-shaped regions. Exact closed-form solution and results," *International Journal of Heat and Mass Transfer*, **46**, pp. 1455–1469 (2003).
21. De Monte, F., "Multi-layer transient heat conduction using transition time scales," International journal of thermal sciences, **45**, pp. 882–892 (2006).
22. Salt, H., "Transient conduction in a two-dimensional composite slab—I. Theoretical development of temperature modes," *International Journal of Heat and Mass Transfer*, **26**, pp. 1611–1616 (1983).
23. Salt, H., "Transient conduction in a two-dimensional composite slab—II. Physical interpretation of temperature modes" *International Journal of Heat and Mass Transfer*, **26**, pp. 1617–1623 (1983).
24. Miller, J. and Weaver, P., "Temperature profiles in composite plates subject to time-dependent complex boundary conditions," *Composite Structures*, **59**, pp. 267–278 (2003).
25. Blanc, M. and Touratier, M., "An efficient and

https://doi.org/10.1017/jmech.2018.54 Published online by Cambridge University Press

simple refined model for temperature analysis in thin laminated composites," *Composite Structures*, **77**, pp. 193–205 (2007).

26. Hsieh, M.H. and Ma, C.C., "Analytical investigations for heat conduction problems in anisotropic thin-layer media with embedded heat sources," *International Journal of Heat and Mass Transfer*, **45**, pp. 4117–4132 (2002).
27. Ma, C.C. and Chang, S.W., "Analytical exact solutions of heat conduction problems for anisotropic multi-layered media," *International Journal of Heat and Mass Transfer*, **47**, pp. 1643–1655 (2004).
28. Norouzi, M., Rahmani, H., Birjandi, A.K. and Joneidi, A.A., "A general exact analytical solution for anisotropic non-axisymmetric heat conduction in composite cylindrical shells," *International Journal of Heat and Mass Transfer*, **93**, pp. 41–56 (2016).
29. Kayhani, M., Norouzi, M. and Delouei, A.A., "A general analytical solution for heat conduction in cylindrical multilayer composite laminates," *International Journal of Thermal Sciences*, **52**, pp. 73–82 (2012).
30. Kayhani, M., Norouzi, M. and Delouei, A.A., "An exact solution of axi-symmetric conductive heat transfer in cylindrical composite laminate under the general boundary condition," *International Journal of Mechanical and Mechatronics Engineering*, **4**, pp. 776–783 (2010).
31. Kayhani, M., Norouzi, M. and Delouei, A.A., "On heat conduction problem in multi–layer composite pin fins," *3th International Conference of Advanced Composite Materials Engineering*, Brasov, Romani, pp. 89–94 (2010).
32. Delouei, A.A., Kayhani, M. and Norouzi, M., "Exact analytical solution of unsteady axi-symmetric conductive heat transfer in cylindrical orthotropic composite laminates," *International Journal of Heat and Mass Transfer*, **55**, pp. 4427–4436 (2012).
33. Tarn, J.Q., "Exact solutions for functionally graded anisotropic cylinders subjected to thermal and mechanical loads," *International Journal of Solids and Structures*, **38**, pp. 8189–8206 (2001).
34. Tarn, J.Q. and Wang, Y.M., "End effects of heat conduction in circular cylinders of functionally graded materials and laminated composites," *International Journal of Heat and Mass Transfer*, **47**, pp. 5741–5747 (2004).
35. Singh, S. and Jain, P.K., "Analytical solution to transient heat conduction in polar coordinates with multiple layers in radial direction," *International journal of thermal Sciences*, **47**, pp. 261–273 (2008).
36. Jain, P.K. and Singh, S., "An exact analytical solution for two-dimensional, unsteady, multilayer heat conduction in spherical coordinates," *International Journal of Heat and Mass Transfer*, **53**, pp. 2133–2142 (2010).
37. Kayhani, M., Shariati, M., Norouzi, M. and Demneh, M.K., "Exact solution of conductive heat transfer in cylindrical composite laminate," *Heat and mass transfer*, **46**, pp. 83 (2009).
38. Norouzi, M., Niya, S.R., Kayhani, M.H., Shariati, M., Demneh, M.K. and Naghavi, M.S., "Exact solution of unsteady conductive heat transfer in cylindrical composite laminates," *Journal of Heat Transfer*, **134**, pp. 101301 (2012).
39. Noruozi, M., Delouei, A.A. and Seilsepour, M., "general exact solution for heat conduction in multilayer spherical composite laminates," *Composite Structures*, **106**, pp. 288–295 (2013).
40. Norouzi, M. and Rahmani, H., "On exact solutions for anisotropic heat conduction in composite conical shells," *International Journal of Thermal Sciences*, **94**, pp. 110–125 (2015).
41. Norouzi, M. and Rahmani, H., "An exact analysis for transient anisotropic heat conduction in truncated composite conical shells," *Applied Thermal Engineering*, **124**, pp. 422-431 (2017).
42. Ozisik, M.N., *Heat conduction*, 2nd edition, John Wiley & Sons, Canada (1993).
43. Myint-U, T. and Debnath, L., "Linear partial differential equations for scientists and engineers," *Springer Science & Business Media*, (2007).
44. Abramowitz, M. and Stegun, I.A., Handbook of mathematical functions: with formulas, graphs, and mathematical tables, Vol. 9, Dover, New York, (1972).
45. Chattopadhyay, S., Pressure vessels: design and practice, 1st edition, *CRC press*, Boca Raton (2004).
46. Aleck, B.J., *Filament wound spherical pressure vessel*, in, Google Patents, (1972).
47. Howell, J.R., Menguc, M.P. and Siegel, R., *Thermal radiation heat transfer*, 5th edition, *CRC press*, Boca Raton (2010).
48. Windhorst, T. and Blount, G., "Carbon-carbon composites: a summary of recent developments and applications," *Materials & Design*, **18**, pp. 11–15 (1997).
49. Touloukian, Y.S., Powell, R., Ho, C. and Klemens, P., *Thermophysical Properties of Matter-The TPRC Data Series*, Volume 2. Thermal Conductivity-Nonmetallic Solids, in, Thermophysical and Electronic Properties Information Analysis Center Lafayette In, (1971).

(Manuscript received December 25, 2017,
accepted for publication September 25, 2018.)

https://doi.org/10.1017/jmech.2018.54 Published online by Cambridge University Press